ChemPlusChem

A Multidisciplinary Journal Centering on Chemistry

Chemistry Europe

European Chemical Societies Publishing

Accepted Article

Title: Self-Assembled Quaternary Ammonium-Containing Comb-Like Polyelectrolytes for the Hydrolysis of Organophosphorous Esters: Effect of Head Groups and Counter-Ions

Authors: Tatiana N. Pashirova, Petr Fetin, Alexey A. Lezov, Matvey V. Kadnikov, Farida G. Valeeva, Evgenia A. Burilova, Alexander Yu. Bilibin, and Ivan M. Zorin

To be cited as: *ChemPlusChem* 10.1002/cplu.202000417

Link to VoR: https://doi.org/10.1002/cplu.202000417

WILEY-VCH

Self-Assembled Quaternary Ammonium-Containing Comb-Like Polyelectrolytes for the Hydrolysis of Organophosphorous Esters: Effect of Head Groups and Counter-Ions

Dr., Tatiana N. Pashirova,*[a] Dr., Petr A. Fetin,*[b] Dr., Alexey A. Lezov,[c] Matvey V. Kadnikov,[b] Dr., Farida G. Valeeva,[a] Dr., Evgenia A. Burilova,[a] Prof., Alexander Yu. Bilibin,[b] Dr., Ivan M. Zorin*[b]

[a] Dr., Tatiana N. Pashirova, Dr., Farida G. Valeeva, Dr., Evgenia.A. Burilova,
Arbuzov Institute of Organic and Physical Chemistry, FRC Kazan Scientific Center, Russian Academy of Sciences,
Arbuzov St., 8, Kazan, 420088, Russian Federation
E-mail: tatyana_pashirova@mail.ru

[b] Dr., Petr A. Fetin, Dr., Ivan M. Zorin, Matvey V. Kadnikov, Prof., Alexander Yu. Bilibin
Institute of Chemistry
St. Petersburg State University,
7/9 Universitetskaya nab, St. Petersburg 199034, Russian Federation
E-mail: p.fetin@spbu.ru, i.zorin@spbu.ru

[c] Dr., Alexey A. Lezov
Department of Molecular Biophysics and Polymer Physics, Physical Faculty
St. Petersburg State University,
7/9 Universitetskaya nab, St. Petersburg 199034, Russian Federation

Supporting information for this article is given via a link at the end of the document

Abstract: The aim of this work was to increase the efficiency of catalytic systems for the hydrolytic cleavage of 4-nitrophenyl esters of phosphonic acids. Quaternary ammonium-containing comb-like polyelectrolytes («polymerized micelles») with ester cleavable fragments and a low aggregation threshold were used as catalysts. The synthesis of poly(11-acryloyloxyundecylammonium) surfactants with different counterions (Br^-, NO_3^-, $CH_3C_6H_4SO_3^-$) and head groups was realized by micellar free-radical polymerization. Molecular weight, critical association concentration, particle sizes and solubilization properties toward Orange OT were determined. Self-assemblies organized by poly(11-acryloyloxyundecyltrimethyl ammonium) bromide successfully catalyze hydrolysis of 4-nitrophenyl butylchloromethylphosphonate up to two orders of magnitude compared to aqueous alkaline hydrolysis. The development of these catalysts is promising for industrial applications and organophosphorus compound detoxification.

Introduction

Self-assembled systems have wide applications in biomimetic and sensor system technologies, protective coatings, nanocontainers.[1–4] Possible applications of self-assemblies results from self-organization in solution and at interfaces and their ability to solubilize organic compounds. One of perspective trends of self-assemblies is their use for studies of different types of organic reactions.[5–8] These catalytic self-assembled nanoreactors lead to design environmentally friendly catalysts and develop green reactions in water.[9–11] Nanocompartments such as micelles,[5,12–14] polymersomes[15] have been established as smart and compact devices to carry out reactions. Catalytic acceleration of chemical reactions in surfactant solutions is caused by micelle formation and transfer of reagents and substrates in micellar pseudophase.[16] Catalytic efficacy is determined by optimization of molecular structure (charge and structure of amphiphilic molecule head group and chain length[17–19]), concentration and type of self-assemblies (micelles, rods, vesicles etc.).[20–23] Cationic surfactants are the most promising due to the charge of head group for biological applications,[3] environmental issues (extractants and flocculants)[24–26] and as catalysts in nucleophilic substitution reaction for hydrolysis of ester bonds.[17,27,28] Reactions of nucleophilic substitution in phosphorus esters play an important role in biological processes.[29] Also, poisoning and pollution by organophosphorus pesticides[30] and insecticides poses serious health problems,[31] environmental problems in water and soils.[32] Therefore, their decomposition is relevant.[33,34] Actual research directions in this area are improvement in the efficacy of catalytic systems and the use of environmentally friendly processes. The latter can be achieved by using green solvents,[35,36] biodegradable surfactants,[37] α-nucleophilic systems[38] and lowering surfactant concentration. It can be achieved by using dimeric (gemini) or polymeric surfactants that have much lower critical micelle concentration (CMC) and higher binding constants than monomeric surfactants.[39,40] The use of polymers as catalysts reduces their concentrations and bring reaction centers much closer.[41][42] Thus, these polymers become closer to enzymatic model of catalysis.[43–46] Design of new hybrid polymers with incorporated and covalent linked reagents within their structure is a way to create a second-generation micellar nanoreactor.[47–49] In this paper we describe synthesis of comb-like polyelectrolyte and their properties related to catalytic hydrolysis of alkylphosphoric acid esters (OP). The reaction of hydrolysis of model organophosphorus substrates 4-nitrophenyl esters of phosphonic acids was examined (Scheme 1a). The so-called «polymerized micelles» are comb-like polyelectrolytes obtained from corresponding micelle-forming monomers. The term was initially used in work[50] and there are numerous examples of such polymers,[51,52] used for waste water treatment, micellar chromatography.

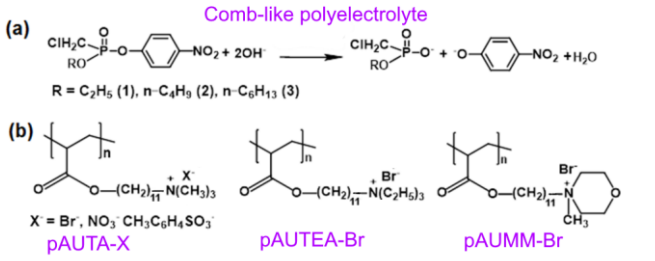

Scheme 1. Hydrolysis of organophosphorus substrates **1-3** in the presence of comb-like polyelectrolytes: pAUTA-X$^-$, pAUTEA-Br$^-$, pAUMM-Br$^-$.

As it was shown in work,[53] there are no direct correlation between shape and size of «polymerized micelles» self-assemblies and shape and size of the parent monomer micelles. These are separate class of surfactants with distinct differences from the monomeric ones. Molecular architecture of most «polymerized micelles» correspond to comb-like type polyelectrolyte. We use three cationic micelle-forming monomers 11-acryloyloxyundecyltrimethylammonium bromide (AUTA-Br), 11-acryloyloxyundecyltriethylammonium bromide (AUTEA-Br) and N-(11-acryloyloxyundecyl)-N-methylmorpholinium bromide (AUMM-Br) to obtain a series of polymers with ester cleavable fragments depicted in Scheme 1b. Systematic study was performed on the influence of structure and counter-ions of micellar surfactants on the nucleophilic cleavage of OP[54,55] but a limited content is available for polymeric surfactants. The present work was initiated to use new type of cleavable «polymerized micelles» with a low aggregation threshold as a catalysts and to expand results about their influence on the nucleophilic cleavage of OPs. Influence of the head group types, counter-ions and degree of polymerization of the comb-like polyelectrolytes were investigated.

Results and Discussion

Polymerization

Micelle forming monomers undergo fast and quantitative conversion to polymer during polymerization in solution at concentrations higher than CMC. The polymerization mechanism is close to microemulsion regime. Conductance measurements were convenient for monitoring the polymerization process[56] (Fig. 1). As the polymerization proceeds, conductance of solution gradually decreased and after polymerization completion, conductance becomes constant. The causes for the conductance decrease are increase in solution viscosity, dramatic decrease of charge carrier number and their mobility. It may take from 10 to 15 minutes to achieve 95-98% conversion.[57] Only monomer molecules incorporated into the micelles undergo fast conversion to polymer, reaction of monomer in molecular solution proceeds much slowly, so theoretical value of conversion (p) may be calculated as fraction of total amount of monomer incorporated in micelles p=(C-CMC)/C.

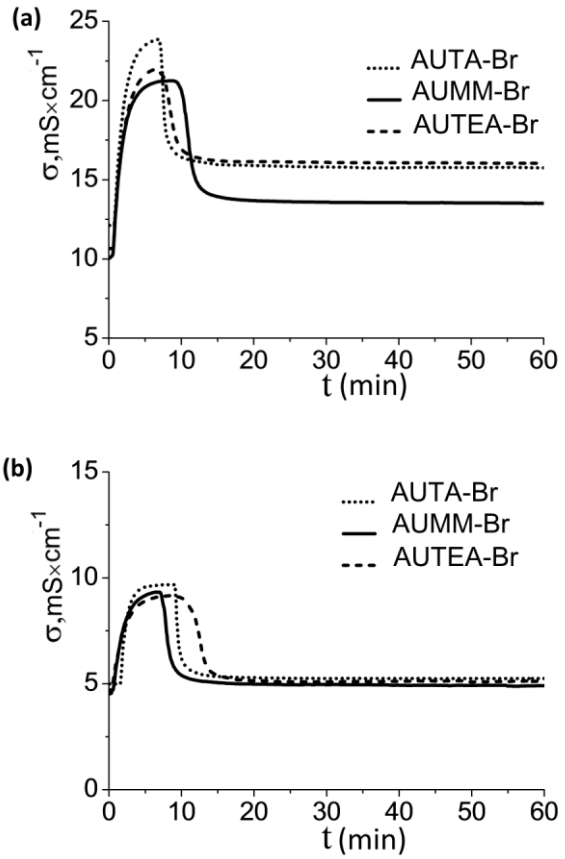

Figure 1. Change in conductance of reaction mixture in the course of polymerization AUTA-Br (short dots), AUMM-Br (solid), AUTEA-Br (short dash) at 60°C and monomer concentration: C=0.27 M (a), C= 0.07M (b).

Thus we obtained a set of polymers with degree of polymerization (DP) ranging from 35 to 230. Determination of molecular weight of the polymers was a special task because of their high adsorptive properties and ability to form associates. Thus, common methods as GPC and SLS appeared to be inapplicable. Average molecular weights ($M_{D\eta}$) of polymers were estimated from viscometry and DLS measurements in 0.05 M aqueous NaCl (See supplementary Fig. s1-s3). The obtained characteristics of investigated comb-like polyelectrolytes are presented in Table 1.

Table 1. Average molecular weights ($M_{D\eta}$), degree of polymerization (DP), self-diffusion coefficients ($D^1{}_0$), intrinsic viscosity ([η]), the jump in conductivity during polymerization (Δσ), and monomers concentration (C_m) during polymerization for comb-like polyelectrolytes.

Monomer	C_m (M)	Δσ (mS·cm^{-1})	[η] (dL·g^{-1})	$D^1{}_0\times10^7$ (cm^2·s^{-1})	$M_{D\eta}\times10^{-3}$	DP
AUTA-Br	0.07	4.4	0.36	4.6	35	100
-	0.27	8.0	1.38	2.2	83	230
AUMM-Br	0.07	4.3	0.53	5.6	13	35
-	0.27	7.6	1.26	2.2	91	220
AUTEA-Br	0.07	4.0	0.50	3.9	41	100
-	0.27	5.8	0.76	3.1	55	135

The $M_{D\eta}$ for pAUTA-Br sample is correlated with molecular weight measured by sedimentation analysis in our previous work.[58] The transient jump in conductivity during polymerization (Δσ, Fig. 1, Table 1) can serve as simple criteria of reproducibility of polymerization. The Δσ value is decreased with decreasing averaged molecular weights of comb-like polyelectrolyte. Ion exchange of Br^- to NO_3^- and Br^- to toluene-4-sulfonate allows to obtain polymers pAUTA-NO_3 and pAUTA-Ts having exactly the same DP as parent pAUTA-Br. Polymers pAUTEA-Br and pAUMM-Br have slightly different DP due to different micellar order in monomer solution in the course of polymerization.

Self-assembly and solubilization properties

The concept of «polymerized micelles» in contrast to common micelles of low-molecular weight compounds contemplates that micelles can exist in full concentration range up to very high dilutions. Nevertheless, formation of hydrophobic domains in solutions of «polymerized micelles» starts at certain concentration – critical association concentration (CAC)[52,59]. The polymers are able to form self-assemblies of two types – intra-macromolecular associates and inter-macromolecular (multi-macromolecular) associates that can be detected by appropriate methods. Solubilization of hydrophobic dyes is an informative method for CAC determination and detection of hydrophobic domains of polymers. Orange OT was used as a spectral probe for determination of CAC and solubilization properties. The absorption spectra of Orange OT in different concentrations polymer solutions are shown in supplementary Fig. s4, s5. Concentration dependences of solution optical densities at λ_{max} = 495 nm (Orange OT adsorption) are shown in Figure 2. Linear increase in optical density corresponding to Orange OT solubilization starts at very low polymer concentration (CAC1). Solubilization capacity (S) evaluated by equation 4 is presented in Table 2. Likely, CAC1 corresponds to the formation of intramolecular self-assemblies. The S of polymeric surfactant at CAC1 corresponds to the solubilization of Orange OT by single macromolecules (S1) (Table 2). CAC2 and S2 correspond to the formation and the solubilization by multi-macromolecular self-assemblies. Effect of the nature of counterions on solubilization properties is observed in Fig. 2A.

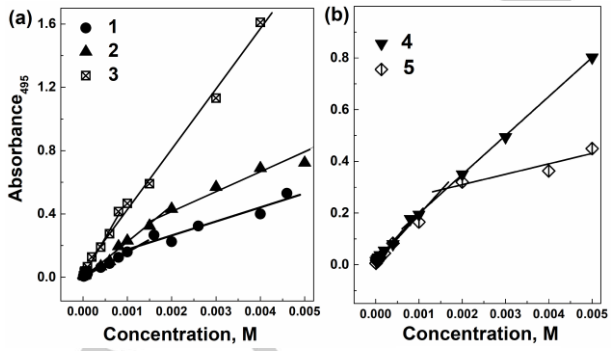

Figure 2. Orange-OT optical density in solutions of pAUTA-Br (1), pAUTA-NO_3 (2), pAUTA-Ts (3) (a) and pAUTEA-Br (4) with DP =100, pAUMM-Br (5) with DP = 35 (b) ,λ_{max} = 495 nm, L=1 cm, 25 ° C.

Table 2. CAC values determined by fluorimetry in the presence of pyrene and spectrophotometry using Orange OT and solubilization capacity (S), 25 ºC

Polyelectrolyte	DP	I_1/I_3 Ratio	CAC[a] (mM)	CAC1[b] (mM)	S1 10^3	CAC2[b] (mM)	S2 10^3
pAUTA-Br	100	1.61-1.55	0.15	0.01	8.4	1.2	4.7
-	230	1.6-1.5	0.24	0.01	13	1.5	17
pAUTA-NO_3	100	1.62	0.02	0.01	11	1.7	6.8
-	230	1.19	0.22	0.01	8.8	0.6	4.9
pAUTA-Ts	100	1.56-1.52	0.03	0.01	26	0.6	20
-	230	1.12	0.04	0.01	35	0.6	15
pAUTEA-Br	100	1.71-1.61	0.2	0.01	11	0.7	8.1
-	135	1.69-1.61	0.1	0.01	17	0.45	4.6
pAUMM-Br	35	1.58-1.51	0.06	0.01	9.8	1.5	2.1

[a] fluorimetry. [b] spectrophotometry using Orange OT.

The solubilization capacity of both intra-macromolecular and inter-macromolecular self-assemblies increased 3 and 4 times, respectively, in the sequence of counterions Br^-<NO_3^-<Ts^-. The highest Orange OT solubilization was achieved for pAUTA-Ts. This S1 value is 1.6 times higher than for CTAB micelles (S = 15.9[60]). The same effect was observed for pAUTA-Ts with DP = 230 (See supplementary Fig. s6). Usually, the replacement of bromide by a hydrophobic anion such as tosylate decreases critical micelle concentration and induces the sphere-to wormlike micelle transition in aqueous solutions of trimethylammonium surfactants.[61] Thus, the improvement in solubilization properties of tosylate ion is mainly due to a change in morphology and a stronger interaction of counterion with surfactant head group.[57] The effect of variation of head groups is shown in Fig. 2b. pAUTEA-Br has the highest solubilization capacity. This may be due to the greater hydrophobicity to the nonpolar core imparting by ethyl substituents at the nitrogen atom. Pyrene has been extensively used for the study of microheterogeneous systems, such as micellar solution[62,63] and polymers.[64,65] In fluorescence emission spectra of pyrene, intensity ratio I_1/I_3 - where I_1 (373 nm) and I_3 (384 nm) - is characteristic of microenvironment polarity of pyrene.[62,63,66] Fig. s7 and s8 in supplementary show pyrene emission spectra in polymer solutions at different concentrations. We can see a shift in the band at low concentrations (0.02-0.2 mM). These changes accompany the transfer of pyrene molecules from water environment to the hydrophobic micellar core. The increase in the intensity of pyrene fluorescence with increasing polymer concentration was also observed.[67,68] This suggests that pyrene was transferred from aqueous to hydrophobic phase. The incorporation of pyrene into micelles appears to suppress the molecular motion of pyrene, resulting in decrease in thermal deactivation of electronically excited state.[69] Dependences of pyrene intensity ratio I_1/I_3 on the polymer concentration are presented in Figure 3. As a rule, this ratio is between 1.6 and 1.9 in aqueous or similarly polar environment.[63,70] For regular polymer micelles, the less polar environment of the core results in a characteristic decrease of the I_1/I_3 ratio. Namely, at high polymer concentration the limiting value of I_1/I_3 represents the polarity sensed by pyrene in the hydrophobic sites of polymer micelle.[68]

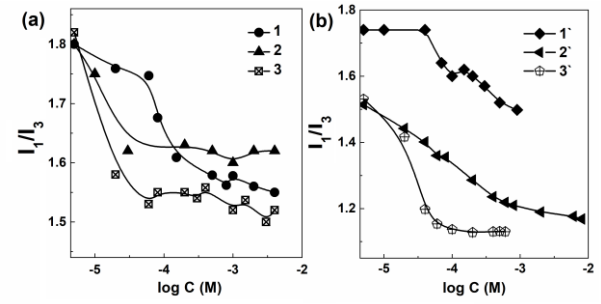

Figure 3. Dependence of intensity ratio (I_1/I_3) of the first and third peaks of pyrene in solutions of pAUTA-Br (1), pAUTA-NO_3 (2), pAUTA-Ts (3) with DP =100 (a) and pAUTA-Br (1`), pAUTA-$NO_3$ (2`), pAUTA-Ts (3`) with DP = 230, 25 °C (b).

For example, I_1/I_3 ≈ 1.38 for polysoap (poly[sodium N-(11-acrylamidoundecanoyl)-L-alaninate),[71] I_1/I_3 ≈ 1.05-1.12 for PS-b-PANa diblock copolymers,[72] I_1/I_3 ≈ 1.2 for Tetronic 908,[73] I_1/I_3 ≈ 1.3 for Pluronic P85,[74] I_1/I_3 ≈ 0.9-1.2 for hydrophobically modified polyacrylates.[75] That is very similar to the micellar environment[76] of ionic detergents (sodium laurate, 1.042; sodium laurylsulfate, 1.136) and nonionic detergents (Triton-X-100, 1.30). Polymers with I_1/I_3 value close to 1.8 and greater were reported in literature.[74,77,78] The plot in Fig. 3a shows that the polarity ratio decreased to 1.5-1.6 for polymer solutions of pAUTA-X with DP=100, which is less than that in water (1.8 or 1.6). Minor but systematic changes in I_1/I_3 values can be interpreted as CAC. The polarity depends on the type of counter-ion and DP. Thus, it is decreasing for pAUTA-X in the order Br^->NO_3^->Ts^- and with increasing DP (Fig. 3B). pAUTA-NO_3 and pAUTA-Ts with DP =230 have the lowest I_1/I_3 value, close to that of solvents such as toluene (1.12) and surfactant (sodium lauryl sulfate). Likely, different polarity is associated with the packing density of polymer chain in self-assemblies. It is consistent with increase in solubilization capacity of polymeric surfactants according to the order pAUTA-Br<pAUTA-NO_3<pAUTA-Ts. It should be noted that an increase in solubilization capacity with growing DP is consistent with decreasing polarity for pAUTA-NO_3 and pAUTA-Ts. It may be stated that pAUTA-Ts has more hydrophobic microdomains to accommodate pyrene and Orange OT inside hydrophobic domain. Hydrophobic probes more easily reach them and penetrates inside. Low solubilization capacity of pAUTA-NO_3 is likely due to the fact that hydrophobic probe Orange OT is located on the periphery of micelles. For pAUTA-Br^-, the I_1/I_3 value is almost equal to 1.6. This corresponds to the location of pyrene probe in polar environment and poor solubilization of Orange OT. The effect of head group of polymeric surfactants slightly changes the polarity. pAUTEA-Br has the highest polarity (Fig. s9). Stepped decreasing polarity is observed with increasing concentration of pAUTEA-Br and pAUMM-Br. The rearrangement of hydrophobic domains structure is observed at 0.1 and 1mM in supplementary Fig. s9. This CAC value (Table 2) is correspond to the interception of the rapidly varying part and the nearly horizontal part at high concentration of the pyrene 1:3 ratio plots (See supplementary Fig. s10, s11). They are in agreement with CAC1 determined by dye solubilization method (Table 2). The CAC of block copolymers are normally much lower than low molecular mass surfactants.[72,79] Low CACs values obtained by dye (Orange OT) solubility method and by

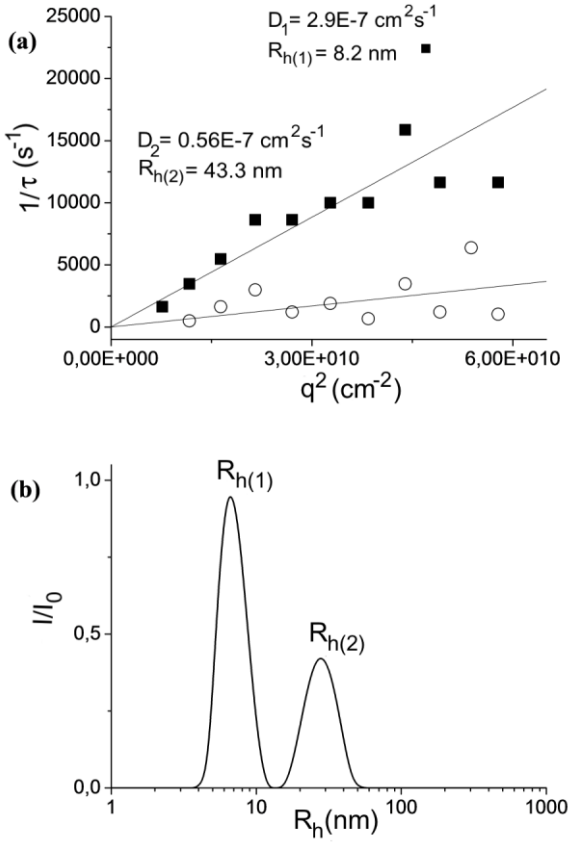

Figure 4. Dependence of the inverse relaxation time (1/τ) on square of wave vector (q^2) (a) and hydrodynamic radius distribution (b) for pAUTA-NO_3 at C= 0.02M.

pyrene fluorescence is fully confirmed by dynamic light scattering. The dependence of the reciprocal of relaxation time (1/τ) on square of wave vector (q^2) passes through the origin for all polymers. This indicates the diffusion nature of observed processes (Fig. 4A and Fig. s2 in supplementary). Determined diffusion coefficients correspond to the two types of polymer particles. DLS data for pAUTA-NO_3 reveal two types of particles, the first one (1-10 nm) corresponds to single macromolecules and the second are multi-macromolecular self-assemblies and the latter appeared to be quite stable under different conditions and dilutions (Fig. 4B). The schematic illustration of the self-assembly process of pAUTA-Br is presented in Scheme 2.

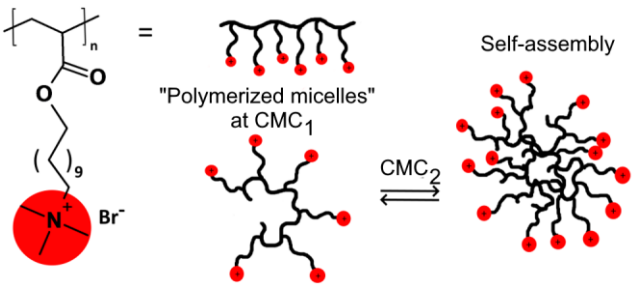

Scheme 2. The schematic illustration of the self-assembly process of comb-like polyelectrolytes pAUTA-Br (short-chain branching is omitted for simplicity).

Unfortunately, DLS data were limited at polymer concentrations lower than CAC2 due to low signal intensity. The number

fraction of these particles can be estimated as 5 %. Zeta-potentials of small particles were positive and fall in range 55-100 mV due to positive charge of head group of polyelectrolytes.

Catalytic properties

As it was shown earlier[80–82] for cationic hydrophobized polymers and surfactants, catalysis is defined by the main contribution of hydrophobic effect. Catalytic effect of polymers on alkaline hydrolysis of different substrates **1-3** (Scheme 1) was investigated by means of spectrophotometric assay of the increase in the absorbance of 4-nitrophenolate anion at 400 nm. Dependence of apparent rate constant (k_{obs}, s^{-1}) for hydrolysis of substrates **1-3** in the presence of comb-like polyelectrolytes are shown in Fig. 5. Increase in rate constant was observed with increasing of polyelectrolyte concentration. There was a tendency of reaching a plateau in the high concentration range, which is typical of micellar catalyzed reactions and suggests binding of substrate to micelles. This allows treating the data in terms of pseudophase model of micellar catalysis, and calculating kinetic parameters of reaction according to equation 7. The calculated parameters for hydrolysis reaction are collected in Table 3. The k_m/k_0 ratio characterizes acceleration of the reaction comparing to reaction in the absence of polymerized catalyst with other conditions being equal. Data for CTAB catalytic effect for the same reaction[81] are given as a reference. From these data it can be seen that catalytic efficiency of comb-like polyelectrolytes depends on DP, type of counterion and head group of polymers. The catalytic effect in the presence of pAUTA-Br is 59, that is two times higher than for classical cationic surfactants CTAB. This effect is most likely determined by high substrate-to-micelle binding constant (2600 M^{-1}) that is two times higher than for CTAB.

Catalytic effect of micelles in micellar catalysis is stipulated by solubilization of substrate molecules and nucleophile. Usually for surfactant micelles, the nucleophile pole is at the periphery of the micelles. This may be affected by the rate of exchange of substrate molecules between solution in micellar pseudophase and by the depth of substrate molecules penetration into the micelle (close to micellar core/center or stay in periphery area). Here we can find the difference between polymerized self-assemblies and micelles of common low molecular weight surfactants known from observations in the field of micellar chromatography.[83] The core of common micelles contains free alkyl tails with relatively loose packing whereas the core of polymerized self-assemblies contains macromolecular chain and alkyl tails attached to it by covalent bonds.[52] So the core of polymerized self-assemblies is denser and have less free volume for solubilization. Consequently, solubilized molecules do not penetrate deep inside the core and locate in peripheral volume of self-assemblies. This causes the faster exchange of solubilizate with solution phase. And this may be one of the possible reasons for increase in the catalytic effect of polymerized surfactants compared to classical surfactants. The increase in catalytic effect can be achieved up to 98 times by changing the head group of polymeric surfactants in the following sequence pAUTA-Br < pAUMM-Br < pAUTEA-Br. This effect is due to an increase in substrate-to-micelle binding constant (Table 3) and solubilization capacity toward to the Orange OT dye (Table 2) in the same sequence.

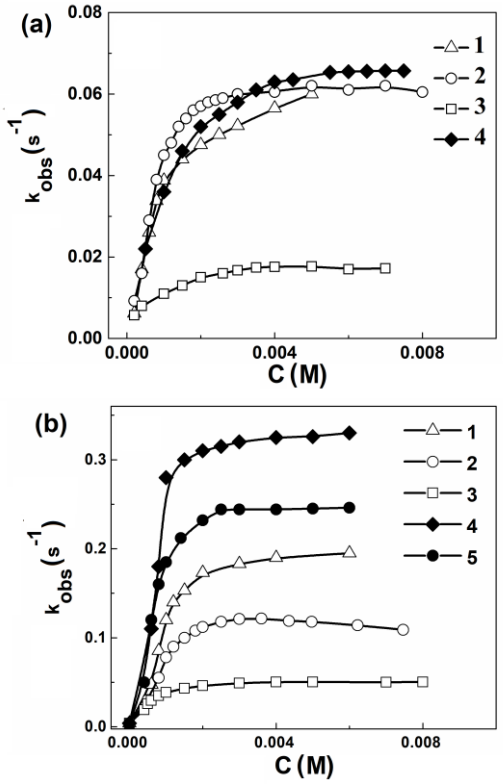

Figure 5. Observed rate constants (k_{obs}, s^{-1}) of hydrolysis of substrates **1** (a) and **2** (b) as functions of polyelectrolyte concentration pAUTA-Br (1), pAUTA-NO_3 (2), pAUTA-Ts (3), pAUTEA-Br (4) with DP = 230 (a), DP=100 (b) pAUMM-Br (5), with DP = 35, 25˚C

Table 3. Kinetic parameters of the reaction of alkaline hydrolysis of substrates **1-3** catalyzed by polymeric surfactants, 25˚C

Polyelectrolyte	DP	Substrate	k_m, s^{-1}	K_S, M^{-1}	CAC×10^3 M	k_m/k_0[a]
pAUTA-Br	100	**2**	0.21	2600	0.5	59
-	230	**1**	0.06	2000	0.25	15
-	230	**2**	0.38	1400	0.1	107
pAUTA-NO_3	100	**2**	0.146	1800	0.4	41
-	230	**1**	0.07	224	0.3	17.5
pAUTA-Ts	100	**1**	0.025	1660	0.3	6
-	100	**2**	0.054	2900	0.25	15
-	100	**3**	0.082	4100	0.1	27
-	230	**1**	0.02	1600	0.1	5
pAUTEA-Br	100	**2**	0.35	3800	0.5	98
-	135	**1**	0.079	941	0.17	20
pAUMM-Br	35	**2**	0.282	2700	0.3	79
CTAB		**2**	0.099	1200	0.46	28

[a] catalytic effect.

The catalytic effect in the case of pAUTA-Br is two times higher with increase in the degree of polymerization from 100 to 230 and reaches 107 times. Catalytic effect of polymer surfactants with Br^- counterion appeared to be four times higher than with $CH_3C_6H_4SO_3^-$.

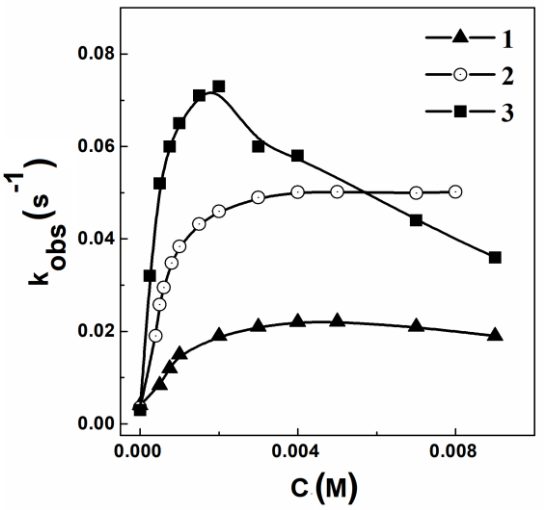

Figure 6. Observed rate constants (k_{obs}, s^{-1}) of hydrolysis of different substrates **1** (1), **2** (2), **3** (3) as a function of polyelectrolyte concentration pAUTA-Ts DP=100, 25°C.

Decrease of reaction rate in a row pAUTA-Br>pAUTA-NO_3>pAUTA-Ts may be caused by decrease in binding constant of nucleophile(OH^-)-to-micelle while binding constants substrate-to-micelle in that cases are rather comparable. The solubilization capacity of these polymeric surfactants toward the hydrophobic dye Orange OT increases in the same sequence. Likely, in the case of toluene-4-sulfonate counterion, more loose micelles are formed. It can be hypothesized that bulky and hydrophobic toluene-4-sulfonate ions screen micelle surface and push off hydroxide anions from the proximity of micelle. This was confirmed by the lowest polarity of pAUTA-Ts seen by the fluorescence of pyrene (Table 2). Some substrate specificity was observed for pAUTA-Ts (Fig. 6). Catalytic effect of micellar polyelectrolyte pAUTA-Ts increased from 6-fold to 27-fold when changing from less hydrophobic phosphonate **1** to more hydrophobic **3** (Table 3). This effect is determined by increase in substrate-to-micelle binding constant from 1660 M^{-1} to 4100 M^{-1} on increasing substrate hydrophobicity. It should be noted that the CAC values determined from kinetic experiment are close to the CAC obtained by Orange OT and pyrene solubilization experiments (Table 2). In addition, the latter confirms that the catalysis of the hydrolysis reaction occurs due to self-assemblies of comb-like polyelectrolytes.

Conclusion

The investigated comb-like polyelectrolyte can form intra-macromolecular and inter-macromolecular self-assemblies with increasing their concentration. The formation of intra-macromolecular self-assemblies starts at extremely low polymer concentrations, the inter-macromolecular self-assembly formation begins at concentration comparable with CMC for typical cationic surfactant (CTAB). Solubilization capacity of the comb-like polyelectrolyte is higher than CTAB and increases with increasing hydrophobicity of ionic groups of polyelectrolytes and counterions. Self-assembly-forming polyelectrolytes exhibit higher catalytic activity for hydrolysis of 4-nitrophenyl esters of phosphonic acids than CTAB. The catalytic efficiency depends on the structure of polyelectrolyte head-group, degree of polymerization and type of counterion. The highest catalytic effect (two orders of magnitude) was observed for hydrolysis of 4-nitrophenyl butylchloromethylphosphonate in the presence of polymer of acryloyl-oxyundecylthriethylammonium bromide. It was 3.5 fold higher than for common CTAB micellar systems. Catalytic activity can be controlled by the molecular weight of polymers and the substrate lipophilicity. New type of cleavable comb-like polyelectrolytes with a low aggregation threshold can be recommended as high potential catalysts for nucleophilic cleavage of OPs. Such catalysts would be of paramount interest for degradation of OPs under mild conditions.

Experimental Section

Chemicals

1-(o-Tolylazo)-2-naphthol (75%, Orange OT, Aldrich, USA), pyrene (99%, Sigma, Switzerland), 11-Bromoundecanol (98%, Aldrich), 2,2'-azobis(2-methylpropionamidine)dihydrochloride (AAPH, 97%, Aldrich), 4-toluenesulfonic acid (monohydrate) (Vekton, Russia), sodium nitrate (Vekton, Russia) were used as received. The substrates **1-3** were prepared according to the procedure.[84] Organic solvents were purified according to standard methods of purification.[85] Purified water (18.2 MΩ), resistivity at 25 °C) from Direct-Q 5 UV equipment (Millipore S.A.S. Molsheim-France) was used for all sample preparations.

Synthesis

11-acryloyloxyundecylbromide: 11-Bromoundecanol (3g) was dissolved in freshly distilled N-methylpyrrolidone (25mL) and cooled to about -10°C. To this solution, cold freshly distilled acryloyl chloride (15% excess) was quickly added, and the reaction mixture was allowed to stay for two days at -18°C. After that, the reaction mixture was poured into 200 mL of icy HCl (0.5M) and extracted 3 times with petroleum ether; combined extracts were dried over sodium sulfate. The 11-acryloyloxyundecylbromide was isolated as slightly yellowish oil (2.7g, 74%) and used in the next steps without additional purification.

11-Acryloyloxyundecyltrimethylammonium bromide (AUTA-Br): AUTA-Br was obtained by reaction of 11-acryloyloxyundecylbromide (2.7g) with trimethylamine (0.68g, 30% excess) in acetonitrile solution (25mL) for 24h at room temperature. After solvent evaporation, the resulting AUTA-Br was purified by crystallization from methanol-acetone mixture. The product was obtained in a yield of 2.4g (74%). The structure of AUTA-Br was confirmed by ^{1}H NMR (See supplementary Fig. s12).

11-Acryloyloxyundecyltriethylammonium bromide (AUTEA-Br): AUTEA-Br obtained according to the above procedure from 11-acryloyloxyundecylbromide (2.7g) with triethylamine (1.16g, 30% excess) at 80°C, 72h under argon in a sealed tube. Resulted AUTEA-Br was washed by hexane, and purified by crystallization from methanol-acetone mixture. The product was obtained in a yield of 2.7g (75%).The structure of AUTA-Br was confirmed by ^{1}H NMR (See supplementary Fig. s13)

N-(11-Acryloyloxyundecyl)-N-methylmorpholinium bromide (AUMM-Br): AUMM-Br according to the above procedure from 11-acryloyloxyundecylbromide (2.7g) with N-methylmorpholine (1.16g, 30% excess) at 80°C 72h under argon in a sealed tube. Resulted AUMM-Br was washed by hexane, and purified by crystallization from methanol-acetone mixture. The product was obtained in a yield of 2.5g (70%). The structure of AUTA-Br was confirmed by ^{1}H NMR (See supplementary Fig. s14)

Polymerization

Polyelectrolyte pAUTA-Br was obtained by free-radical polymerization of the corresponding monomer at concentration 0.07M and 0.27M (Those concentrations correspond 4×CMC of AUTA-Br and 16×CMC of AUTA-Br) in water under argon atmosphere using AAPH initiator (1 gL^{-1}) at 60 °C for 1h under control of conductance measurements. The resulting polymers were dialyzed against water (cellulose membrane tube with molecular weight cut-off 14000 (Sigma-Aldrich D9652) was used for dialysis). The yields of the polymers after purification and isolation were about 90%. The structure of pAUTA-Br samples and impurities absents were checked by ^{1}H NMR. All other polyelectrolytes (pAUTEA-Br pAUMM-Br) were obtained according to the above procedure; the yields of polymers after purification were not less 90%. pAUTA-NO_3 and pAUTA-Ts were prepared by dialysis of pAUTA-Br solution against sodium nitrate or sodium toluene-4-sulfonate in water followed by dialysis against water and freeze-drying.[86] pAUTA-Br samples with DP 100 and 230 were used for this transformation to obtain two series of pAUTA-X polymers, where DP is the degree of polymerization.

Viscometry

Viscometric measurements were conducted on a Lovis 2000 M rolling ball microviscometer (Anton Paar, Austria) at 25°C in a 0.05 M aqueous NaCl or water. The intrinsic viscosity [η] was calculated from Huggins and Cramer plots[87] by linear extrapolation of concentration dependence of $\eta_{sp}c^{-1}$.

DLS study

DLS measurements were performed with PhotoCor Complex (Photocor Instruments Inc., Russia) instrument equipped with real-time correlator (288 channels, 10 ns) in scattering angle range 30-140° at 25±0.1°C, with laser light source having wavelength, λ=405 nm. Autocorrelation functions of scattered light intensity was processed using DynaLS software (providing the distributions of scattered light intensity and, therefore, distributions of relaxation times τ). The dependence between 1/τ and the square of the scattering vector:

$$q = \frac{4\pi\eta_0}{\lambda}\sin\left(\frac{\theta}{2}\right) \quad (1)$$

The dependence between 1/τ and the square of the scattering for all studied samples was a line passing through the origin, indicating the diffusional character of the observed processes (See supplementary Fig. S2)[88] (otherwise results were discarded). Hydrodynamic radii were calculated using Stokes-Einstein equation $D=k_BT\times(6\pi\eta_oR_h)^{-1}$, where η_0-dynamic viscosity of solvent; R_h – hydrodynamic radius; k_B - Boltzmann constant; T - absolute temperature. Translational diffusion coefficient D was calculated from the slope of this line according to the following relationship.

$$\frac{1}{\tau} = Dq^2 \quad (2)$$

for both single macromolecules (D_1) and polymer self-assemblies (D_2) for each investigated concentration (Table s1). The self-diffusion coefficient (D_0) was calculated by linear extrapolation of concentration dependencies of translation diffusion coefficients (D) (See supplementary Fig. S3). All samples were centrifuged to remove dust before investigation.

Molecular weight

Average molecular weights ($M_{D\eta}$) of the comb-like polymers were estimated from viscometry and DLS measurements in 0.05 M aqueous NaCl according to (3)

$$M_{D\eta} = \left(\frac{A_0T}{\eta D_0}\right)^3 \frac{1}{[\eta]} \quad (3)$$

where A_0 - hydrodynamic invariant (A_0= 3.2×10^{-10}, erg×mol^{-1}×K^{-1}, this value is typically for flexible and comb-like macromolecules)[89]; T – Absolute temperature, K; η – viscosity of solvent, Pa·s; D_0 -self-diffusion coefficients, cm^{2}s^{-1}; $[\eta]$ – intrinsic viscosity, cm^{3}g^{-1}.

Spectrophotometry (dye solubilization)

Solubilization of the dye (Orange OT) was performed by adding an excess of crystalline Orange OT to the polymeric surfactant solutions. These solutions were allowed to equilibrate for about 48 h at constant temperature, followed by filtration. Then the absorbance was measured at 495 nm (Orange OT), using the spectrophotometer Specord 250 Plus (Analytik Jena AG, Germany). Quartz cuvettes (L = 1 cm) containing sample were used. Solubilization capacity of associates (S), which corresponds to the number of moles of dye solubilized per mole of surfactant was determined according to equation 4[90]

$$S = \frac{B}{\varepsilon_{ext}\times L} \quad (4)$$

where B is the slope of dye absorbance as a function of surfactant at concentration above CMC and ε_{ext} the extinction coefficient of Orange OT (ε_{ext} = 18720 M^{-1} cm^{-1}).[91]

Fluorescence

Fluorescence spectra of pyrene (1×10^{-6} M) in water solutions of cationic surfactants were recorded at constant temperature on a Varian Cary Eclipse spectrofluorimeter (Varian, Inc., California, USA) with excited wavelength for pyrene at 335 nm, using 1 cm path length quartz cuvettes. Emission spectra were recorded in the 350-500 nm range. Fluorescence intensities of the first peak at 373 nm (I_1), of the third peak at 384 nm (I_3), and of the peak at 394 nm were determined from the spectra. The pyrene 1:3 ratio plots were approximated by a decreasing sigmoid of Boltzmann type, which is given by equation 5[76]

$$\frac{I_1}{I_3} = \frac{A_1-A_2}{1+\exp\left(\frac{C-C_0}{\Delta C}\right)} + A_2 \quad (5)$$

Where A_1 and A_2 - upper and lower bounds of I_1/I_3;C- surfactant concentration, M;C_0 and ΔC - approximation parameters;The CAC value was determined as CAC = C_0 + 2ΔC. This CAC value corresponds to the interception of the rapidly varying part and the nearly horizontal part at high concentration of the pyrene 1:3 ratio plots (See supplementary Fig. s10, s11).

Kinetic study

The reaction was monitored by following the release of the p-nitrophenolate anion absorption at 400 nm. The UV spectra were measured on Specord 250 Plus (Analytik Jena AG, Germany) spectrophotometer. The spectra of surfactants were determined at least three times, they were reproducible, and average parameters were taken into account. The oscillator strength was calculated on the basis of the integral intensity of the corresponding absorption band. The observed rate constants for the reaction (k_{obs}, s^{-1}) were determined by the first-order equation (6):

$$\lg(D_\infty - D_t) = -0.434k_{obs}t + const \quad (6)$$

where D_∞ and D_t are absorbance after completion of the reaction and at a time point t, respectively. The concentrations of substrates **1-3** were $5\cdot10^{-5}$—$1\cdot10^{-4}$ mol L^{-1}, the concentration of NaOH was 0.001 M, T=25˚C

Each k_{obs} value is the mean of at least three independent determinations differing by no more than 4%. The parameters of the micelle-catalyzed process were determined by equations of the pseudophase model of micellar catalysis.[16,92,93]. This kinetics obeys a formalism similar to the Michaelis−Menten equation for enzyme catalysis (7)

$$k_{obs} = \frac{k_m K_S\left(C_{surf} - CMC\right) + k_0}{1 + K_S\left(C_{surf} - CMC\right)} \quad (7)$$

where K_S is the binding constant of the substrate, k_o and k_m(s^{-1}) are the pseudo-first-order rate constants in water and catalytic complexes, respectively. CMC is critical micelle concentration. In the case of polymer and polymer—colloidal systems the term critical association concentration (CAC) is usually used.

Acknowledgements

Fetin P.A. and Kadnikov M.V. are grateful to RSF Grants № 19-73-00059 for synthesis of comb-like polyelectrolyte and investigation of polyelectrolyte solution in St. Petersburg State University. The work (solubilization and catalytic properties of the polymers) of T.N. Pashirova, F.G. Valeeva, E.A. Burilova, was financial support from the government assignment for FRC Kazan Scientific Center of Russian Academy of Sciences. The authors are indebted to Prof. L.Ya. Zakharova who initiated this work. They express to her their thanks for her interest and constant support.

Keywords: hydrolysis • phosphorous acid esters • polyelectrolytes •self-assembly • surfactants

[1] S. Chakraborty, S. Varghese, S. Ghosh, *Chem. - A Eur. J.* **2019**, *25*, 16725–16731.

[2] T. N. Pashirova, I. M. Zorin, A. Y. Bilibin, L. Y. Zakharova, A. I. Konovalov, *Russ. Chem. Bull.* **2016**, *65*, 268–272.

[3] L. Y. Zakharova, T. Pashirova, S. Doktorovova, A. R. Fernandes, E. S. López, A. M. Silva, S. B. Souto, E. B. Souto, *Int. J. Mol. Sci.* **2019**, *20*, 5534.

[4] R. R. Kashapov, A. M. Bekmukhametova, K. A. Petrov, I. R. Nizameev, M. K. Kadirov, L. Y. Zakharova, *Sensors Actuators, B Chem.* **2018**, *273*, 592–599.

[5] T. Dwars, E. Paetzold, G. Oehme, *Angew. Chemie - Int. Ed.* **2005**, *44*, 7174–7199.

[6] B. Samiey, C. H. Cheng, J. Wu, *J. Chem.* **2014**, *2014*, 908476.

[7] T. N. Ansari, F. Gallou, S. Handa, in *Organomet. Chem. Ind. A Pract. Approach* (Eds.: T.J. Colacot, C.C.C.J. Seechurn), Wiley-VCH Verlag GmbH & Co. KGaA, **2020**, pp. 203–238.

[8] F. Gallou, B. H. Lipshutz, in *Organometallics Process Chem.* (Eds.: T.J. Colacot, V. Sivakumar), Springer, Cham, **2018**, pp. 199–216.

[9] C. Risi, M. Calamante, E. Cini, V. Faltoni, E. Petricci, F. Rosati, M. Taddei, *Green Chem.* **2020**, *22*, 327–331.

[10] P. Cotanda, A. Lu, J. P. Patterson, N. Petzetakis, R. K. O'Reilly, *Macromolecules* **2012**, *45*, 2377–2384.

[11] P. Qu, M. Kuepfert, S. Jockusch, M. Weck, *ACS Catal.* **2019**, *9*, 2701–2706.

[12] B. H. Lipshutz, S. Ghorai, M. Cortes-Clerget, *Chem. - A Eur. J.* **2018**, *24*, 6672–6695.

[13] G. La Sorella, G. Strukul, A. Scarso, *Green Chem.* **2015**, *17*, 644–683.

[14] M. Cortes-Clerget, N. Akporji, J. Zhou, F. Gao, P. Guo, M. Parmentier, F. Gallou, J. Y. Berthon, B. H. Lipshutz, *Nat. Commun.* **2019**, *10*, 2169.

[15] P. Tanner, P. Baumann, R. Enea, O. Onaca, C. Palivan, W. Meier, *Acc. Chem. Res.* **2011**, *44*, 1039–1049.

[16] I. V Berezin, K. Martinek, A. K. Yatsimirskii, *Russ. Chem. Rev.* **1973**, *42*, 787–802.

[17] X. Han, V. K. Balakrishnan, E. Buncel, *Langmuir* **2007**, *23*, 6519–6525.

[18] S. M. K. Reddy, J. Kothandapani, M. Sengan, A. Veerappan, S. Selva Ganesan, *Mol. Catal.* **2019**, *465*, 80–86.

[19] Z. Hafidi, M. Ait Taleb, A. Amedlous, M. El Achouri, *Catal. Letters* **2019**, *150*, 1309–1324.

[20] N. J. Buurma, *Curr. Opin. Colloid Interface Sci.* **2017**, *32*, 69–75.

[21] M. N. Khan, M. H. R. Azri, *J. Phys. Chem. B* **2010**, *114*, 8089–8099.

[22] Y. L. Sim, N. S. M. Yusof, A. Ariffin, M. Niyaz Khan, *J. Colloid Interface Sci.* **2011**, *360*, 182–188.

[23] J. Li, Z. Lin, Q. Huang, Q. Wang, L. Tang, J. Zhu, J. Deng, *Green Chem.* **2017**, *19*, 5367–5370.

[24] X. Liu, J. Wang, E. Liu, T. Yang, R. Li, Y. Sun, *Sci. Total Environ.* **2020**, *710*, 136346.

[25] J. Zhong, W. Guan, C. Lu, *Green Chem.* **2018**, *20*, 2290–2298.

[26] Y. Zhou, Y. J. S. Lai, E. Eustance, L. Straka, C. Zhou, S. Xia, B. E. Rittmann, *Water Res.* **2017**, *126*, 189–196.

[27] M. L. Satnami, S. Dhritlahre, R. Nagwanshi, I. Karbhal, K. K. Ghosh, F. Nome, *J. Phys. Chem. B* **2010**, *114*, 16759–16765.

[28] D. K. Dubey, A. K. Gupta, M. Sharma, S. Prabha, R. Vaidyanathaswamy, *Langmuir* **2002**, *18*, 10489–10492.

[29] W. W. Cleland, A. C. Hengge, *Chem. Rev.* **2006**, *106*, 3252–3278.

[30] A. Singh, P. Raj, N. Kaur, N. Singh, *Detoxification and Sensing of Organophosphate-Based Pesticides and Preservatives in Beverages*, Elsevier Inc., **2019**.

[31] M. Eddleston, N. A. Buckley, P. Eyer, A. H. Dawson, **2008**, *371*, 597–607.

[32] J. Muff, L. MacKinnon, N. D. Durant, L. F. Bennedsen, K. Rügge, M. Bondgaard, K. D. Pennell, *Environ. Sci. Pollut. Res.* **2020**, *27*, 3428–3439.

[33] K. Kim, O. G. Tsay, D. A. Atwood, D. G. Churchill, *Chem. Rev.* **2011**, *111*, 5345–5403.

[34] S. F. d. A. Cavalcante, A. B. C. Simas, M. C. Barcellos, V. G. M. de Oliveira, R. B. Sousa, P. A. d. M. Cabral, K. Kuča, T. C. C. França, *Biomolecules* **2020**, *10*, 1–22.

[35] P. Pavez, G. Oliva, D. Millán, *ACS Sustain. Chem. Eng.* **2016**, *4*, 7023–7031.

[36] M. Oyarzun, G. Oliva, R. D. Falcone, P. Pavez, *ACS Sustain. Chem. Eng.* **2020**, *8*, 5478–5484.

[37] S. J. Pandya, I. V. Kapitanov, Z. Usmani, R. Sahu, D. Sinha, N. Gathergood, K. K. Ghosh, Y. Karpichev, *J. Mol. Liq.* **2020**, *305*, 112857.

[38] N. Singh, Y. Karpichev, A. K. Tiwari, K. Kuca, K. K. Ghosh, *J. Mol. Liq.* **2015**, *208*, 237–252.

[39] B. Kumar, D. Tikariha, K. K. Ghosh, *J. Mol. Liq.* **2014**, *193*, 243–248.

[40] D. R. Gabdrakhmanov, E. A. Vasilieva, M. A. Voronin, D. A. Kuznetsova, F. G. Valeeva, A. B. Mirgorodskaya, S. S. Lukashenko, V. M. Zakharov, A. R. Mukhitov, D. A. Faizullin, et al., *J. Phys.*

Chem. C **2020**, *124*, 2178–2192.
[41] L. A. Giusti, M. Medeiros, N. L. Ferreira, J. R. Mora, H. D. Fiedler, *J. Phys. Org. Chem.* **2014**, *27*, 297–302.
[42] X. Ma, L. Zhang, M. Xia, X. Zhang, Y. Zhang, *J. Hazard. Mater.* **2018**, *355*, 65–73.
[43] A. K. Andrianov, Y. A. Osinkin, V. Y. Igonin, N. A. Platé, *Polym. Sci. U.S.S.R.* **1991**, *33*, 1006–1012.
[44] R. S. Mello, E. S. Orth, W. Loh, H. D. Fiedler, F. Nome, *Langmuir* **2011**, *27*, 15112–15119.
[45] A. P. Gerola, E. H. Wanderlind, Y. S. Gomes, L. A. Giusti, L. García-Río, R. A. Nome, A. J. Kirby, H. D. Fiedler, F. Nome, *ACS Catal.* **2017**, *7*, 2230–2239.
[46] E. Kuah, S. Toh, J. Yee, Q. Ma, Z. Gao, *Chem. - A Eur. J.* **2016**, *22*, 8404–8430.
[47] M. K. Škopić, K. Götte, C. Gramse, M. Dieter, S. Pospich, S. Raunser, R. Weberskirch, A. Brunschweiger, *J. Am. Chem. Soc.* **2019**, *141*, 10546–10555.
[48] K. P. Sullivan, W. A. Neiwert, H. Zeng, A. K. Mehta, Q. Yin, D. A. Hillesheim, S. Vivek, P. Yin, D. L. Collins-Wildman, E. R. Weeks, et al., *Chem. Commun.* **2017**, *53*, 11480–11483.
[49] L. Zhang, S. L. Baker, H. Murata, N. Harris, W. Ji, G. Amitai, K. Matyjaszewski, A. J. Russell, *Adv. Sci.* **2020**, *7*, 1–10.
[50] A. J. Hyde, D. J. M. Robb, *J. Phys. Chem.* **1963**, *67*, 2089–2092.
[51] S. Hamid, D. Sherrington, *J. Chem. Soc. Chem. Commun.* **1986**, 936–938.
[52] C. M. Paleos, C. I. Stassinopoulou, A. Malliaris, *J. Phys. Chem.* **1983**, *87*, 251–254.
[53] D. Cochin, F. Candau, R. Zana, *Macromolecules* **1993**, *26*, 5755–5764.
[54] B. Kumar, M. L. Satnami, K. K. Ghosh, K. Kuca, *J. Phys. Org. Chem.* **2012**, *25*, 864–871.
[55] N. S. M. Yusof, M. N. Khan, *Adv. Colloid Interface Sci.* **2013**, *193–194*, 12–23.
[56] I. M. Zorin, T. M. Shcherbinina, E. I. Demidov, E. V. Mechtaeva, N. A. Zorina, P. A. Fetin, A. Y. Bilibin, *Colloid Polym. Sci.* **2019**, *297*, 1169–1176.
[57] P. A. Fetin, I. M. Zorin, A. A. Lezov, V. I. Fetina, A. Y. Bilibin, *J. Mol. Liq.* **2020**, *309*, 113103.
[58] N. V. Tsvetkov, P. A. Fetin, A. A. Lezov, A. S. Gubarev, L. I. Achmadeeva, A. A. Lezova, I. M. Zorin, A. Y. Bilibin, *J. Mol. Liq.* **2015**, *211*, 239–246.
[59] E. D. Sprague, D. C. Duecker, C. E. Larrabee, *J. Am. Chem. Soc.* **1981**, *103*, 6797–6800.
[60] T. N. Pashirova, A. S. Sapunova, S. S. Lukashenko, E. A. Burilova, A. P. Lubina, Z. M. Shaihutdinova, T. P. Gerasimova, V. I. Kovalenko, A. D. Voloshina, E. B. Souto, et al., *Int. J. Pharm.* **2020**, *575*, 118953.
[61] R. Abdel-Rahem, *Adv. Colloid Interface Sci.* **2008**, *141*, 24–36.
[62] K. Kalyanasundaram, J. K. Thomas, *J. Am. Chem. Soc.* **1977**, *99*, 2039–2044.
[63] D. C. Dong, M. A. Winnik, *Photochem. Photobiol.* **1982**, *35*, 17–21.
[64] O. Anthony, R. Zana, *Macromolecules* **1994**, *27*, 3885–3891.
[65] F. Petit-Agnely, I. Iliopoulos, R. Zana, *Langmuir* **2000**, *16*, 9921–9927.
[66] L. Piñeiro, M. Novo, W. Al-Soufi, *Adv. Colloid Interface Sci.* **2015**, *215*, 1–12.
[67] Y. Li, K. Nakashima, *Langmuir* **2003**, *19*, 548–553.
[68] A. F. Olea, P. Silva, I. Fuentes, F. Martínez, D. R. Worrall, *J. Photochem. Photobiol. A Chem.* **2011**, *217*, 49–54.
[69] K. Nakashima, P. Bahadur, *Adv. Colloid Interface Sci.* **2006**, *123–126*, 75–96.
[70] A. V. Kabanov, I. R. Nazarova, I. V. Astafieva, E. V. Batrakova, V. Y. Alakhov, A. A. Yaroslavov, V. A. Kabanov, *Macromolecules* **1995**, *28*, 2303–2314.
[71] R. R. Nayak, S. Roy, J. Dey, *Polymer (Guildf).* **2005**, *46*, 12401–12409.
[72] I. Astafieva, X. F. Zhong, A. Eisenberg, *Macromolecules* **1993**, *26*, 7339–7352.
[73] J. Puig-Rigall, I. Obregon-Gomez, P. Monreal-Pérez, A. Radulescu, M. J. Blanco-Prieto, C. A. Dreiss, G. González-Gaitano, *J. Colloid Interface Sci.* **2018**, *524*, 42–51.
[74] R. Luxenhofer, A. Schulz, C. Roques, S. Li, T. K. Bronich, E. V. Batrakova, R. Jordan, A. V. Kabanov, *Biomaterials* **2010**, *31*, 4972–4979.
[75] L. Aricov, A. Băran, E. L. Simion, I. C. Gîfu, D. F. Anghel, V. V. Jerca, D. M. Vuluga, *Colloid Polym. Sci.* **2016**, *294*, 667–679.
[76] J. Aguiar, P. Carpena, J. A. Molina-Bolívar, C. Carnero Ruiz, *J. Colloid Interface Sci.* **2003**, *258*, 116–122.
[77] M. M. Lübtow, L. C. Nelke, J. Seifert, J. Kühnemundt, G. Sahay, G. Dandekar, S. L. Nietzer, R. Luxenhofer, *J. Control. Release* **2019**, *303*, 162–180.
[78] F. M. Winnik, S. T. A. Regismond, *Colloids Surfaces A Physicochem. Eng. Asp.* **1996**, *118*, 1–39.
[79] D. V. Pergushov, E. V. Remizova, M. Gradzielski, P. Lindner, J. Feldthusen, A. B. Zezin, A. H. E. Müller, V. A. Kabanov, *Polymer (Guildf).* **2004**, *45*, 367–378.
[80] L. Y. Zakharova, A. R. Ibragimova, F. G. Valeeva, A. V. Zakharov, A. R. Mustafina, L. A. Kudryavtseva, H. E. Harlampidi, A. I. Konovalov, *Langmuir* **2007**, *23*, 3214–3224.
[81] L. Y. Zakharova, T. N. Pashirova, R. R. Kashapov, E. P. Zhil'Tsova, N. K. Gaisin, O. I. Gnezdilov, A. B. Konov, S. S. Lukashenko, I. M. Magdeev, *Kinet. Catal.* **2011**, *52*, 179-185.
[82] S. S. Lukashenko, A. V. Yurina, T. N. Pashirova, D. B. Kudryavtsev, E. M. Kosacheva, L. A. Kudryavtseva, A. I. Konovalov, *Colloid J.* **2008**, *70*, 317-326.
[83] J. Wang, I. M. Warner, *Anal. Chem.* **1994**, *66*, 3773–3776.
[84] L. C. Kingsland, *Law Contemp. Probl.* **1948**, *13*, 354.
[85] A. Y. Bilibin, T. M. Shcherbinina, N. V. Girbasova, V. T. Lebedev, Y. V. Kulvelis, V. S. Molchanov, I. M. Zorin, *Des. Monomers Polym.* **2016**, *19*, 369–380.
[86] P. A. Fetin, I. M. Zorin, E. V. Mechtaeva, D. A. Voeiko, N. A. Zorina, D. A. Gavrilova, A. Y. Bilibin, *Eur. Polym. J.* **2019**, *116*, 562–569.
[87] R. Pamies, J. G. Hernández Cifre, M. del Carmen López Martínez, J. García de la Torre, *Colloid Polym. Sci.* **2008**, *286*, 1223–1231.
[88] P. E. R. Cummins H. Z., Ed. , in *Phot. Correl. Light Beating Spectrosc.*, Springer, Boston, MA, **1974**.
[89] V. Tsvetkov, *Rigid-Chain Polymers*, **1989**.
[90] J. R. McElhanon, T. Zifer, S. R. Kline, D. R. Wheeler, D. A. Loy, G. M. Jamison, T. M. Long, K. Rahimian, B. A. Simmons, *Langmuir* **2005**, *21*, 3259–3266.
[91] H. Schott, *J. Phys. Chem.* **1967**, *71*, 3611–3617.
[92] C. A. Bunton, G. Savelli, *Adv. Phys. Org. Chem.* **1986**, *22*, 213–309.
[93] E. J. Fendler, J. H. Fendler, *Adv. Phys. Org. Chem.* **1970**, *8*, 271–406.

10.1002/cplu.202000417

Entry for the Table of Contents

Insert graphic for Table of Contents here.

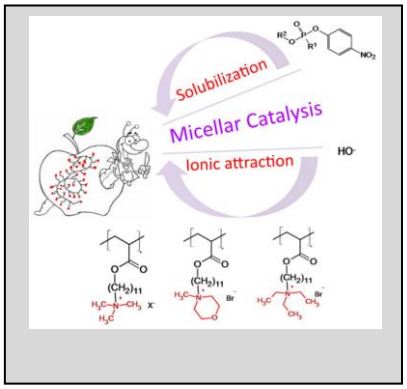

Self-assemblies of cationic comb-like polyelectrolytes with a low association threshold were used as catalysts for alkali hydrolysis of phosphorous acid esters. The catalytic effect is up to two orders of magnitude compared to aqueous alkaline hydrolysis. The polyelectrolytes can be recommended as high potential catalysts for degradation of OPs under mild conditions.